

Physical properties and structure of glass medium QS-P₂O₅-CaO-BaO-Gd₂O₃/GdF₃ doped Dy³⁺

Maranata Sri Rejeki Simanjuntak¹, Elyzabeth Simanullang¹, Juniar Hutahae¹,
 Zulkarnain², Juniastel Rajagukguk^{1,*}

¹Department of Physics, Universitas Negeri Medan, Deli Serdang 20221, Indonesia

²Department of Physics, Universitas Riau, Pekanbaru 28293, Indonesia

Corresponding author: juniastel@unimed.ac.id

ABSTRACT

Optical glass medium derived from local natural resources, namely Huta Ginjang quartz sand was successfully synthesized using the melt-quenching method at a temperature of 1200°C. The chemical composition of the glass was arranged in the main formulation of 15QS + 59.5 P₂O₅ + 5 CaO + 10 BaO + 5 Gd₂O₃/GdF₃ + 0.5 Dy₂O₃ with active ion doping Dy³⁺ at a concentration of 3 mol%. The main difference between the two samples lay in the substitution of Gd₂O₃ with GdF₃ which produced two types of samples with different characteristics. After the initial stage of formation, the samples were cut and polished to obtain precise dimensions and the appropriate level of transparency. Characterization tests included measuring density, molar volume and ion concentration based on the Archimedes principle as well as numerical calculations. Structural analysis was carried out using Fourier transform infrared spectroscopy (FTIR) to identify the constituent functional groups and X-ray diffraction (XRD) to ensure the amorphous nature of the glass medium. This research was conducted to develop locally sourced phosphate glass materials as potential candidates for optical media applications in photonics technology.

Keywords: Dy³⁺; FTIR; Gd³⁺; optical media; quartz sand

Received 04-09-2025 | Revised 17-11-2025 | Accepted 24-11-2025 | Published 30-11-2025

INTRODUCTION

In the last decade, phosphate-based glass materials have attracted much attention for research as host media in optical applications because they have open network properties, low phonon energy, and high doping ability to rare earth ions [1-3]. Phosphate glass systems have advantages in terms of ease of processing, good thermal and chemical stability, and high compatibility with various types of dopants [4, 5]. The combination of phosphate with quartz sand (QS) as a local source of SiO₂ from Huta Ginjang, is able to produce superior quality glass matrices that have competitive economic value [5, 6]. The use of rare earth ions such as Dysprosium (Dy³⁺) in glass media has shown great potential in producing strong spectral emissions in the blue and yellow bands. This can make it an ideal candidate for white lighting applications and as an optic [7-9]. To improve the performance of silica-phosphate

glass media, it can be done by adding compounds such as BaO and CaO as network modifiers. While Gd₂O₃ and GdF₃ function as energy donors in the Dy³⁺ codoping system [10, 11]. Phosphate (P₂O₅) has the ability to form flexible polymeric structures, assist in the addition of active ions, and lower the phonon energy of the host medium [10, 12]. Low phonon energy is very important for the luminescence process because it can reduce non-radiative losses, which increases the quantum efficiency of emission from rare earth ions doped into the matrix [13, 14]. Dy³⁺ ions have characteristic transitions of ⁴F_{9/2} → ⁶H_{15/2} and ⁴F_{9/2} → ⁶H_{13/2}, which are very important for white light (LED) applications based on color mixing [13, 15]. The luminescence efficiency of Dy³⁺ is strongly influenced by the local environment of the ion in the glass network, including the field symmetry and the distance between active ions [16, 17]. In co-doping systems using Gd³⁺, Dy³⁺ emission can be

enhanced through $Gd^{3+} \rightarrow Dy^{3+}$ energy transfer [18, 19]. Previous studies, Dy^{3+} doped phosphate glass systems showed sharp emission peaks and good thermal stability [18, 20]. According to Yodkantee et al. that by adding Gd_2O_3 up to 17 mol%, the internal energy transfer capability can increase the scintillation efficiency up to 15.42% [1]. Research by Reddeppa et al. states that the $CaO-P_2O_5-Dy_2O_3$ system has strong emission and long excitation time [21]. Codoping Dy^{3+} with Gd_2O_3 and GdF_3 into the phosphate system provides a significant increase in emission intensity, especially in the yellow band. Energy transfer from Gd^{3+} to Dy^{3+} takes place efficiently, maximizing the radiative transition of Dy^{3+} [14, 22]. The content of GdF_3 contributes to lowering the phonon energy of the environment around Dy^{3+} , which directly reduces non-radiative relaxation [23, 24]. BaO and CaO act as glass network modifiers, which increase the refractive index, density, and strength of the amorphous structure [23, 25]. The addition of Gd_2O_3 strengthens the network through ionic interactions with P_2O_5 and QS, and serves as an energy transfer center to Dy^{3+} . GdF_3 has an important role in stabilizing the network and improving quantum efficiency by lowering the phonon energy [2, 24].

RESEARCH METHODS

Phosphate glass samples with the composition $15QS + 59.5P_2O_5 + 5 CaO + 10 BaO + 5 Gd_2O_3/GdF_3 + 0.5 Dy_2O_3$ and its variations with partial substitution of Gd_2O_3 by GdF_3 were synthesized using the melt-quenching technique. Chemicals in the form of quartz sand QS, P_2O_5 , CaO, BaO, Gd_2O_3/GdF_3 , and Dy_2O_3 were weighed according to the molar composition (20 grams) using a digital scale, then mixed homogeneously in a mortar. The mixture was melted in an alumina crucible at a temperature of about $1200^\circ C$ for 3 hours in an electric furnace, then poured into a preheated stainless steel mold. The annealing process was carried out at $500^\circ C$ for 3 hours to relieve internal stress, then the sample was slowly cooled to room temperature, cut, and polished

to form a glass sample measuring approximately $1\text{ cm} \times 0.2\text{ cm} \times 1.5\text{ cm}$, the amorphous structure was confirmed by X-ray diffraction (Rigaku Miniflex 600). Identification of functional groups was carried out by FTIR spectroscopy (Bruker) in the range of $400 - 4000\text{ cm}^{-1}$.

RESULTS AND DISCUSSION

Medium Glass Display

Samples that have been successfully prepared with a combination of Gadolinium Oxide and Gadolinium Fluoride are shown in Figure 1.

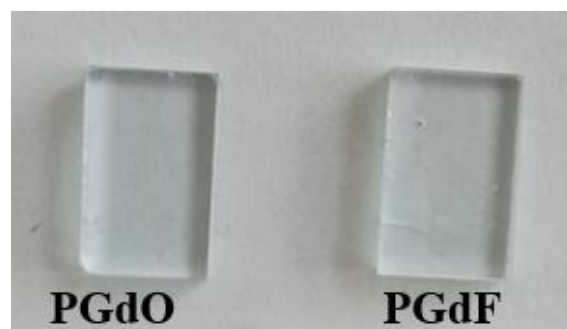


Figure 1. Appearance of PGdO and PGdF glass medium.

The two optical glass samples show differences in appearance, with PGdO exhibiting higher clarity compared to PGdF, which appears somewhat opaque. This is related to the F- anion, which does not always result in increased transparency [11, 26]. The reflectance values between the two samples also differ, with variations in refractive index and density affecting light loss in the samples [15, 17]. The improved transparency of PGdO has positive implications for optical applications because it minimizes scattering and increases transmission efficiency [21, 22].

Physical Properties of Glass Medium

Table 1 below shows the value of each physical parameter of the PGdO and PGdF glass media doped with Dysprosium (Dy^{3+}) ions.

Table 1. Physical properties of PGdO and PGdF glass media.

Physical parameter	Glass sample	
	PCBGO	PCBGEF
Molar weight (g/mol)	129.5365	122.1239
Density (gr/cm ³)	2.8824	2.7833
Molar volume (cm ³ /mol)	44.9405	43.8774
Ion concentration, N × 10 ²² (ion/cm ³)	6,7001	6.8625
Polaron radius × 10 ⁻⁸ (Amstrong)	9.9205	9.8417
Inter nuclear distance × 10 ⁻⁸	2.4621	2.4425
Field strength, F × 10 ¹⁷ cm ²	5.99	6.09
Refractive index (n)	1.5357	1.5403
Molar refractivity (R _m)	14.0066	13.773
Molar electronic polarization × 10 ⁻²⁴	5.5554	5.4627
Metallization criteria (M)	0.6883	0.6861
Reflection loss ρ %	4.4632	4.5238
Dielectric constant (ϵ)	2.3584	2.3725
Thickness (mm)	3	3

Based on the results of the physical properties analysis in Table 1, the molar weight of PGdO was recorded at 129.5365 g/mol, while PGdF was 122.1239 g/mol. In Figure 2 the densities (ρ) were 2.8824 g/cm³ for PGdO and 2.7833 g/cm³ for PGdF, respectively, with the active ion density of PGdO being 6.7001 ions/cm³ and PGdF being 6.8625 ions/cm³. This difference is in line with previous studies showing that the substitution of oxide (Gd₂O₃) with fluoride (GdF₃) affects the total molar mass and network packing, thus directly impacting the density and compactness of the active center [27, 28]. The higher ion density in PGdF indicates an increase in the number of luminescent centers per unit volume, which potentially increases the emission intensity and reabsorption opportunities in optics [29, 30]. The obtained refractive index values ($n(\text{PGdO}) = 1.5357$; $n(\text{PGdF}) = 1.5403$) indicate that PGdF has a slightly higher response to electromagnetic fields, consistent with the

influence of local electron density and anionic composition on polarizability [31, 32]. The molar refractivity of PGdO was recorded at 14.0066 cm³/mol and the electronic polarizability $\alpha_e(\text{PGdO})$ was 5.5554×10^{-24} cm³. This indicates that despite the higher density of PGdO, the specific polarizability value is greater in the oxide variant, which is related to the bonding structure and the contribution of valence orbitals to the field response [33, 3]. The relationship between R_m , n , and α_e in this phosphate medium can be explained using the Lorentz relation and the Clausius Mossotti model [34, 35]. In addition, the low relative dielectric constant values (PGdO = 2.3584; PGdF = 2.3725) and the metallization criteria in the range of 0.686 – 0.688 indicate that both media are still far from the metallic limit and function as electrical insulators. This condition supports the reduction of non-radiative electrical energy dissipation in optics [36, 37]. These parameters also strengthen the stability of the internal field and reduce electronic signal losses [38].

Properties of the Glass Medium Structure

The silicate-phosphate glass network is generally composed of PO₄ tetrahedral units that can be modified by earth metal ions [20, 23, 39]. Modification by Gd₂O₃ and GdF₃ not only affects the local structure, but also impacts the network density and average phonon energy, which have a significant influence on the luminescence performance [10, 28, 40]. Structural characterization was carried out using XRD and FTIR to verify the amorphous nature and the presence of structural functional groups [7, 20].

Fourier Transform Infrared (FTIR)

FTIR spectroscopy analysis was performed on two samples, namely PGdO and PGdF. Figure 3 is the infrared transmittance spectrum (%) in the wavenumber range of 500 – 4000 cm⁻¹.

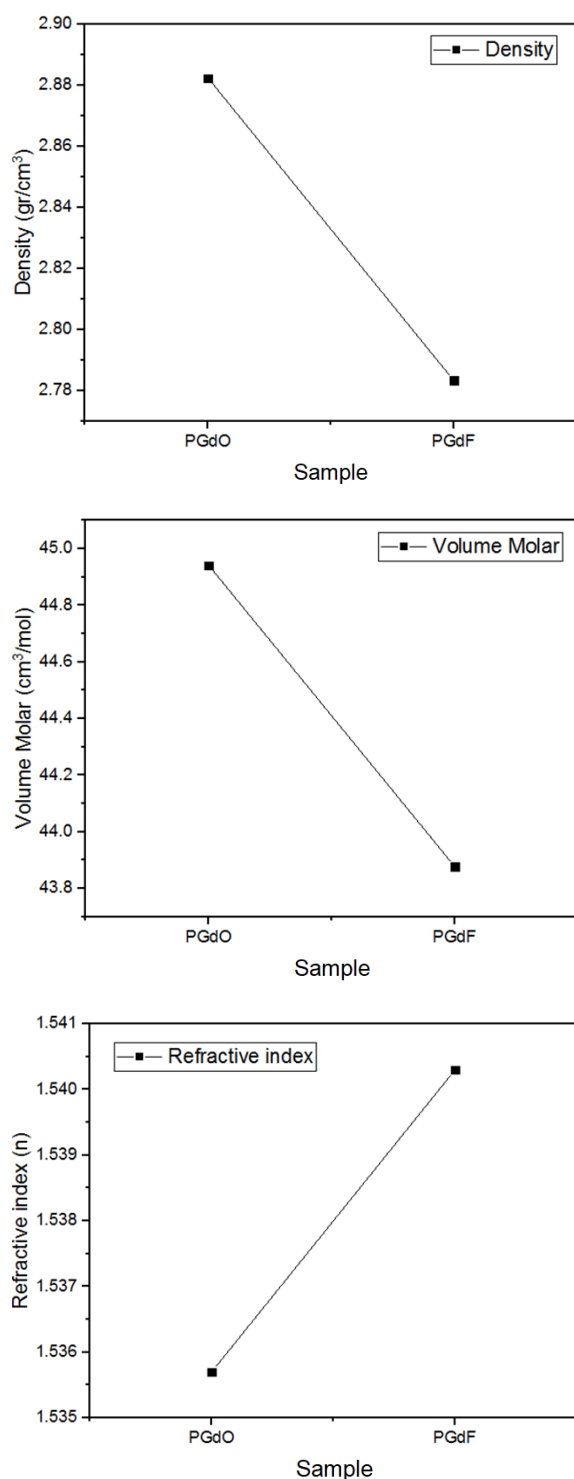


Figure 2. Graph of density, molar volume, and refractive index of PGdO and PGdF glass media.

The broad absorption peaks observed around 3228 cm^{-1} for PGdO and 2886 cm^{-1} for PGdF are associated with stretching vibrations of the hydroxyl (-OH) groups. These groups are generally derived from environmental humidity or residual water trapped during the production

process. The difference in peak positions between the two samples reflects variations in the strength of hydrogen bonding interactions, which are influenced by the chemical composition of each glass, particularly the presence of oxide ions in PGdO and fluoride ions in PGdF. These changes could be an early sign of changes in the local structure around the functional groups, which could then potentially affect the efficiency of energy transfer in optical applications. The absorption in the range of $1633 - 1634\text{ cm}^{-1}$ in both samples is associated with stretching vibrations of the HOH molecules, indicating the presence of free water molecules or residual solvent in the glass network. The presence of excess water or -OH groups is a concern in optics, as it can increase non-radiative energy losses and reduce the efficiency of light emission. The peak observed at wavenumber around 897 cm^{-1} , with more dominant intensity in PGdO, indicates the presence of symmetric POP bonds, which is a characteristic of phosphate network structure. Meanwhile, the absorption around 426 cm^{-1} is attributed to the bending vibration of MO bonds, where M is a metallic element such as Gd^{3+} or F, which contributes to the formation of glass network structure.

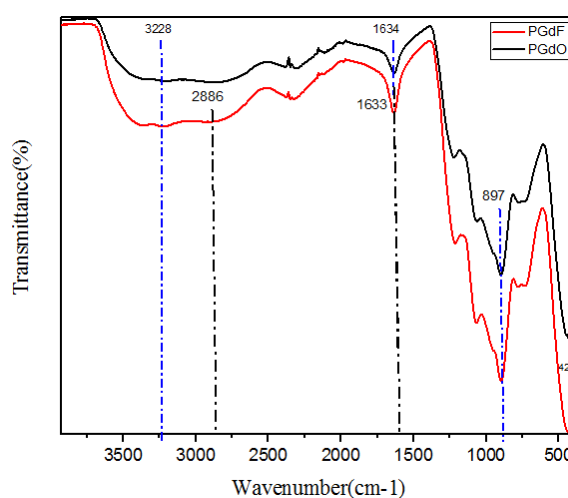


Figure 3. FTIR spectrum of PGdO and PGdF samples.

X-Ray Diffraction (XRD)

XRD diffraction patterns are used to identify the structural properties of a material,

particularly in distinguishing between amorphous and crystalline phases. In glassy materials, which generally lack long-range order, the XRD pattern will show a broad band halo without sharp peaks, indicating amorphous nature. This technique is important to ensure that the glass preparation process successfully produces a medium without significant crystallinity.

Table 2. FTIR spectral peaks of Dysprosium ion-doped glass medium.

Wave number (cm ⁻¹)	Sample	Functional groups
3228	PGdO	-OH stretching
2886	PGdF	-OH stretching
1633 – 1634	Both of them	HOH bending
897	PGdO	Symmetric POP vibration
504	PGdF	Asymmetric PO ₄ ³⁻ bending/POM vibrations
426	Both of them	MO bending(Gd-O, Dy-O, FM)

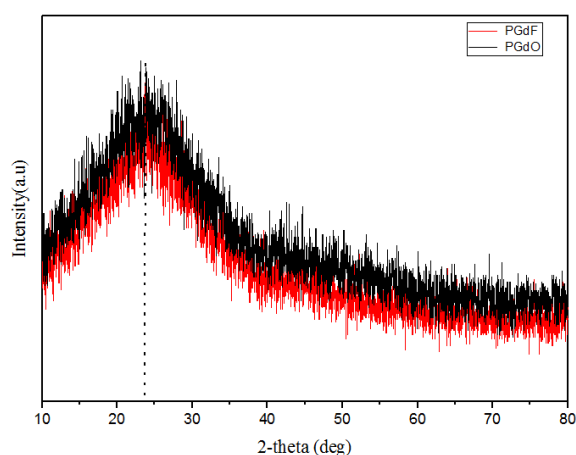


Figure 4. XRD spectrum of PGdF and PGdO glass medium.

Figure 4 shows the X-ray diffraction (XRD) patterns for PGdO and PGdF without any sharp crystalline peaks in the range $2\theta = 20^\circ - 35^\circ$, with the highest peak around 25° , these characteristics confirm the presence of an amorphous phase in both samples [41- 43]. The absence of sharp crystalline peaks is a crucial structural requirement for optical media, as it maintains the homogeneity of the network and

avoids the formation of crystalline domains that can serve as photon scattering centers [44-46]. The interpretation of the hump width refers to the short-range ordering such as the average bond lengths and angles in the PO₄ units that form the phosphate network [47, 48]. The relative difference in hump intensity between PGdO and PGdF (slightly higher intensity in PGdO) is consistent with variations in local atomic density and atomic scattering factors influenced by oxide composition (Gd₂O₃) increasing the scattering contribution compared to fluoride (GdF₃) thereby modulating the amorphous diffraction profile [49, 50]. In addition, substitution of oxide by fluoride tends to change the inter-tetrahedron spacing and local electron distribution, which appears as subtle changes in the position and width of XRD humps [51, 52].

CONCLUSION

This study successfully synthesized a phosphate-silicate glass medium based on Huta Ginjang quartz sand with Dy³⁺ ion doping through the melt-quenching method. Variations in the use of Gd₂O₃ and GdF₃ significantly affected the physical and optical properties, where the addition of GdF₃ decreased the molar mass and density but increased the active ion density and refractive index, while Gd₂O₃ supported structural stability and polarizability. FTIR and XRD analyses confirmed the amorphous nature and changes in chemical bonds due to anion substitution, which implied differences in the degree of polymerization of the glass network. Thus, both types of media showed complementary characteristics: PGdF was more prospective for increasing luminescence intensity, while PGdO provided better network stability. These results confirmed the great potential of Indonesian local resources in the development of phosphate glass-based optical materials, as well as opening opportunities for further research for doping optimization and increasing the efficiency of optoelectronic and radiation applications.

ACKNOWLEDGMENTS

This research was made possible thanks to funding from the Ministry of Education, Culture, Research, and Technology (Kemendikbudristek) through Medan State University. The authors also express their gratitude to Thailand Science Research and Innovation and Nakhon Pathom Rajabhat University for their contributions and support.

REFERENCES

1. Yodkantee, D., Prasatkhetragarn, A., & Kaewkhao, J. (2023). Local structure and energy transfer of Gd^{3+} to Dy^{3+} in phosphate-based glasses. *Radiation Physics and Chemistry*, **209**.
2. Galleani, G., Lodi, T. A., & de Camargo, A. S. (2022). Photoluminescence and X-ray induced scintillation in Gd^{3+} -modified fluorophosphate glasses doped with Ce^{3+} . *Optical Materials*, **133**, 112934.
3. Manyum, P., Rittisut, W., & Kaewkhao, J. (2023). Structural and luminescence properties of transparent borate glass co-doped with Gd^{3+}/Pr^{3+} for photonics application. *Materials Today Communications*, **37**.
4. Ehrt, D. (2015). Phosphate and fluoride phosphate optical glasses--properties, structure and applications. *Physics & Chemistry of Glasses: European Journal of Glass Science & Technology Part B*, **56**.
5. Rajagukguk, J., Simamora, P., & Kothan, S. (2025). NIR luminescence properties of Nd^{3+} ion doped glasses medium based on Huta Gintang quartz sand. *Radiation Physics and Chemistry*, **229**, 112466.
6. Hutahaean, J., Tambunan, F. E. F., & Kaewkhao, J. (2024). Quartz sand "Huta Gintang" on physical properties and structure of phosphate glass medium. *Journal of Physics: Conference Series*.
7. Al-Ghamdi, H., Alfryyan, N., & Mahdy, E. A. (2024). Efficiency of K_2WO_4 containing a newly synthesized phosphate based glasses: Physical, thermal properties, FTIR spectroscopy and γ -ray shielding parameters. *Radiation Physics and Chemistry*, **224**, 112068.
8. Campbell, J. H. (1996). Recent advances in phosphate laser glasses for high-power applications. *Inorganic Optical Materials: A Critical Review*, **10286**, 4–40.
9. Alharshan, G. A., Elamy, M. I., & Said, S. A. (2024). Physical, structural, and optical characteristics of the glasses system based on lanthanum-doped phosphate. *Optical and Quantum Electronics*, **56**(7), 1179.
10. Chen, J., Zhang, X., & Wu, W. (2025). Advances in gadolinium-based composite materials for neutron and gamma-ray shielding. *Frontiers in Materials*, **12**.
11. Grammes, T., de Ligny, D., & Brauer, D. S. (2024). Dispersion, ionic bonding and vibrational shifts in phospho-aluminosilicate glasses. *Physical Chemistry Chemical Physics*, **26**.
12. Griebenow, K., Truong, M. P., & Galusek, D. (2023). Tuning the fluorescence of Dy^{3+} via the structure of borophosphate glasses. *Scientific Reports*, **13**(1), 1919.
13. Dhinakaran, A. P., Vinothkumar, P., & Kalpana, S. (2024). Investigation on luminescent characteristics of Tb^{3+}/Dy^{3+} co-doped boro-phosphate glass for cool white LED and radiation shielding applications. *Applied Physics A*, **130**(10).
14. Hossain, K. M. Z., Patel, U., & Ahmed, I. (2018). Porous calcium phosphate glass microspheres for orthobiologic applications. *Acta Biomaterialia*, **72**, 396.
15. Ntarisa, A. V., Saha, S., & Kaewkhao, J. (2022). Fabrication and investigation of the effects of various gadolinium compounds on Ce^{3+} -activated phosphate glasses for scintillation applications. *Optik*, **262**.
16. Peters, P. M. & Houde-Walter, S. N. (1999). New rare-earth hosts: OH in laser glasses. *Optical Devices for Fiber Communication*, **3847**, 168–179.
17. Marzouk, M. A., ElBatal, H. A., & Ezz-Eldin, F. M. (2019). Collective optical, FTIR, and photoluminescence spectra of CeO_2 and/or Sm_2O_3 -Doped Na_2O - ZnO -

- P₂O₅ Glasses. *International Journal of Optics*, **2019**(1).
18. Goj, P., Wajda, A., & Stoch, P. (2021). Development of a new Sr-O parameterization to describe the influence of SrO on iron-phosphate glass structural properties using molecular dynamics simulations. *Materials*, **14**(15), 4326.
 19. Rajagukguk, J., Sarumaha, C. S., & Kaewkhao, J. (2021). Radio and photo luminescence of Dy³⁺ doped lithium fluorophosphate scintillating glass. *Radiation Physics and Chemistry*, **185**.
 20. Jiménez, J. A., Hedge, V., & Amesimenu, R. (2024). Insights into the structural, thermal/dilatometric, and optical properties of Dy³⁺-doped phosphate glasses for lighting applications. *ACS Physical Chemistry Au*, **4**(6), 720–735.
 21. Reddeppa, T., Krishnaiah, K. V., & Kagola, U. K. (2024). Visible and NIR steady-state luminescence properties of Dy³⁺ ions-doped calcium phosphate glasses for light-emitting diodes. *Materials Today: Proceedings*.
 22. Fang, X., Ray, C. S., & Day, D. E. (2001). Iron redox equilibrium, structure and properties of iron phosphate glasses. *Journal of Non-Crystalline Solids*, **283**.
 23. Galleani, G., Lodi, T. A., & de Camargo, A. S. (2024). Photoluminescence and X-ray induced scintillation in Gd³⁺-Tb³⁺ co-doped fluoride-phosphate glasses, and derived glass-ceramics containing NaGdF₄ nanocrystals. *Optical Materials: X*, **21**.
 24. Ondee, W., Kedkaew, C., & Kaewkhao, J. (2025). Ce³⁺ doped BaO-Gd₂O₃-P₂O₅ glass: New glass scintillator for X-rays detector and imaging applications. *Radiation Physics and Chemistry*, 113205.
 25. Shoaib, M., Rajaramakrishna, R., & Kaewkhao, J. (2020). Structural and luminescence study of Dy³⁺ doped phosphate glasses for solid state lighting applications. *Optical Materials*, **109**.
 26. Basavapoornima, C., Jayasankar, C. K., & Chandrachoodan, P. P. (2009). Luminescence and laser transition studies of Dy³⁺: K-Mg-Al fluorophosphate glasses. *Physica B: Condensed Matter*.
 27. Kaewnuam, E., Wantana, N., & Kaewkhao, J. (2022). The influence of CeF₃ on radiation hardness and luminescence properties of Gd₂O₃-B₂O₃ glass scintillator. *Scientific Reports*, **12**(1).
 28. Khalil, E., El-Damrawi, G., & Moustafa, Y. M. (2025). Optical parameters and shielding attitude of sodium fluoride in calcium-borate glasses. *Optical and Quantum Electronics*, **57**(1), 106.
 29. Dimitrov, V. & Komatsu, T. (2015). Polarizability, basicity and chemical bonding of single and multicomponent oxide glasses. *Journal of Chemical Technology & Metallurgy*, **50**(4).
 30. Li, B. & Zhou, G. (2025). Preparation of phosphate glass by the conventional and microwave melt-quenching methods and research on its performance. *Materials*, **18**.
 31. Amjad, R. J., Sahar, M. R., & Arifin, R. (2013). Synthesis and characterization of Dy³⁺ doped zinc-lead-phosphate glass. *Optical Materials*, **35**(5), 1103–1108.
 32. Shoaib, M., Chanthima, N., & Sangwaranatee, N. (2020). The physical and luminescent properties of Dy³⁺ doped phosphate glasses for solid states lighting applications. *Suranaree J. Sci. Technol*, **27**.
 33. Elisa, M., Sava, B. A., & Abraham, B. (2012). Optical and structural characterization of Eu³⁺, Dy³⁺, Ho³⁺ and Tm³⁺-doped phosphate glasses. *Physics and Chemistry of Glasses-European Journal of Glass Science and Technology Part B*, **53**(5), 219–224.
 34. Hayden, J. S., Hayden, Y. T., & Campbell, J. H. (1990). Effect of composition on the thermal, mechanical, and optical properties of phosphate laser glasses. *High-Power Solid State Lasers and Applications*, **1277**.
 35. Moustafa, E. B., Ghandourah, E. I., & Hammad, A. H. (2022). The effect of V₂O₅ on the BaO-Al₂O₃-P₂O₅ glass for use in optical filters. *Journal of Materials Research and Technology*, **19**, 4905–4914.

36. Li, H., Yi, J., & Liang, X. (2019). Structures, thermal expansion, chemical stability and crystallization behavior of phosphate-based glasses by influence of rare earth. *Journal of Non-Crystalline Solids*, **522**, 119602.
37. Reddy, A. A., Sekhar, M. C., & Prakash, G. V. (2011). Optical properties of Dy³⁺-doped sodium–aluminum–phosphate glasses. *Journal of Materials Science*, **46**.
38. Pinto, I. C., Galleani, G., & de Camargo, A. S. S. (2021). Fluorophosphate glasses doped with Eu³⁺ and Dy³⁺ for X-ray radiography. *Journal of Alloys and Compounds*, **863**, 158382.
39. Schulte, A., Guo, Y., & Cardinal, T. (2008). Low-frequency vibrational excitations in a niobium–phosphate glass for Raman gain applications. *Vibrational Spectroscopy*, **48**.
40. Macedo, A. G., Ferreira, R. A., & Rocha, J. (2010). Effects of phonon confinement on anomalous thermalization, energy transfer, and upconversion in Ln³⁺-doped Gd₂O₃ nanotubes. *Advanced Functional Materials*, **20**(4), 624–634.
41. de Oliveira Jr, M., Gonçalves, T. S., & Eckert, H. (2017). Structure–property relations in fluorophosphate glasses: An integrated spectroscopic strategy. *The Journal of Physical Chemistry C*, **121**.
42. Rada, R., Vermesan, H., & Culea, E. (2023). Development of iron–silicate composites by waste glass and iron or steel powders. *Molecules*, **28**(17), 6296.
43. Lebedev, V. A., Kozlov, D. A., & Garshev, A. V. (2016). The amorphous phase in titania and its influence on photocatalytic properties. *Applied Catalysis B: Environmental*, **195**.
44. Novais, A. L. F., Dantas, N. O., & Vermelho, M. V. D. (2015). Spectroscopic properties of highly Nd-doped lead phosphate glass. *Journal of Alloys and Compounds*, **648**, 338–345.
45. Abbas, J., Zaman, F., & Kaewkhao, J. (2025). Judd-Ofelt (JO) Parameterization: Tuning optical and luminescent features of Dy³⁺-doped phosphate glasses for W-LEDs and laser applications. *Optical Materials*, 117311.
46. Park, J. H., Park, J., & Park, Y. (2020). Disordered optics: exploiting multiple light scattering and wavefront shaping for nonconventional optical elements. *Advanced Materials*, **32**(35).
47. Rao, A. S. (2022). Spectroscopic characterizations of Dy³⁺ ions doped phosphate glasses for epoxy-free white LED applications. *Optical Materials*, **132**.
48. Uskoković, V. (2019). Disordering the disorder as the route to a higher order: incoherent crystallization of calcium phosphate through amorphous precursors. *Crystal Growth & Design*, **19**(8), 4340.
49. Shaar, H. R., Azla, M. N., & Yusof, N. N. (2022). Oxide ion polarizability, optical basicity, and metallization criterion of GO-coated Nd₂O₃ (NPs)-TeO₂ glass for linear optical fibre. *Chalcogenide Letters*, **19**(8).
50. Shoaib, M., Chanthima, N., & Kaewkhao, J. (2019). Physical and luminescence properties of rare earth doped phosphate glasses for solid state lighting applications. *Interdisciplinary Research Review*, **14**(3).
51. Al-Shamiri, H. A. (2025). Structural, physical, and luminescence properties of sodium–aluminum–zinc borophosphate glass embedded with Nd³⁺ ions for optical applications. *Reviews on Advanced Materials Science*, **64**(1), 20250154.
52. Tian, S., Lun, Y., & Yang, Z. (2022). Silicate-clad Dy³⁺ doped multi-component phosphate glass core glass fiber for yellow laser applications. *Journal of Non-Crystalline Solids*, **577**, 121313.



This article uses a license
[Creative Commons Attribution
 4.0 International License](https://creativecommons.org/licenses/by-nc/4.0/)